Identification of 1,3−Dialkylimidazolium Salt Supramolecular Aggregates in Solution

ARTICLE *in* THE JOURNAL OF PHYSICAL CHEMISTRY B · APRIL 2005

Impact Factor: 3.3 · DOI: 10.1021/jp0452709 · Source: PubMed

Identification of 1,3-Dialkylimidazolium Salt Supramolecular Aggregates in Solution

Crestina S. Consorti,[†] Paulo A. Z. Suarez,[†,‡] Roberto F. de Souza,[†] Robert A. Burrow,[§] David H. Farrar,[||] Alan J. Lough,[||] Watson Loh,[⊥] Luis H. M. da Silva,[⊥] and Jairton Dupont*[,†]

Laboratory of Molecular Catalysis, Institute of Chemistry, UFRGS, Av. Bento Gonçalves, 9500 Porto Alegre 91501-970 RS, Brazil, Departamento de Química, UFSM, Santa Maria, RS, Brazil, Department of Chemistry, University of Toronto, Ontario, Canada M5S 3G3, and Instituto de Química, UNICAMP, CP l6154 Campinas 13083-970 SP, Brazil

Received: October 15, 2004; In Final Form: January 7, 2005

The nature of the interactions between 1,3-dialkylimidazolium cations and noncoordinating anions such as tetrafluoroborate, hexafluorophosphate, and tetraphenylborate has been studied in the solid state by X-ray diffraction analysis and in solution by ^{1}H NMR spectroscopy, conductivity, and microcalorimetry. In the solid state, these compounds show an extended network of hydrogen-bonded cations and anions in which one cation is surrounded by at least three anions and one anion is surrounded by at least three imidazolium cations. In the pure form, imidazolium salts are better described as polymeric supramolecules of the type $\{[(DAI)_3(X)]^{2+}[(DAI)(X)_3]^{2-}\}_n$ (where DAI is the dialkylimidazolium cation and X is the anion) formed through hydrogen bonds of the imidazolium cation with the anion. In solution, this supramolecular structural organization is maintained to a great extent, at least in solvents of low dielectric constant, indicating that mixtures of imidazolium ionic liquids with other molecules can be considered as nanostructured materials. This model is very useful for the rationalization of the majority of the unusual behavior of the ionic liquids.

Introduction

Room-temperature ionic liquids (RTILs) emerged at the end of the 1990s as a new and exiting field, opening new horizons for many areas of chemistry, particularly in green chemistry.[1] Imidazolium-based RTILs, such as 1-*n*-butyl-3-methylimidazolium tetrafluoroborate ([BMI]BF_4) and the hexafluorophosphate analogue ([BMI]PF_6),[2] are liquids over a wide temperature range, with negligible vapor pressure, relatively high conductivity, high thermal and relatively good chemical stability,[3] and a wide electrochemical window (up to 7 V).[4] They have been successfully used as media for organic chemistry,[5] organometallic catalysis,[1] electrochemistry,[6] and separation processes,[7] etc. The physical−chemical properties of these ionic liquids (ILs) are strongly influenced by the nature of the *N*-alkyl imidazolium substituents and that of the counteranion.[4,8]

Much research effort has been devoted to the understanding of the role of the different parameters that control the physical−chemical properties of RTILs. Attempts to correlate the strength of the hydrogen bonds between the cation and anion, the length and/or symmetry of the *N*-alkyl imidazolium substituents, and symmetry or size of the anion with the physical−chemical properties (melting point, viscosity, conductivity, etc.) of these materials have displayed only limited trends.[8c] Therefore, knowledge of the structure of these ILs can play an important role in their design and applications.[8c]

More than a decade ago it was proposed that in the solid state 1-ethyl-3-methylimidazolium chloride should be considered as a three-dimensional network of anions and cations linked together by weak interactions (mainly hydrogen bonds), as shown by X-ray crystallographic data.[9] X-ray diffraction studies of cocrystal (imidazolium salt and 1,4-phenylenediamine) indicated that the general pattern of supramolecular organization of the salt part remain the same in the crystal as in the pure IL.[10] It was also suggested by spectroscopic studies that molten and crystalline pure 1-alkyl-3-methylimidazolium salts have a similar structure in both solid and liquid states.[11] In the past decade, several authors observed similar weak interaction networks for imidazolium cation salts. Using NMR and conductivity studies, it was observed that in solution 1-ethyl-3-methylimidazolium halides form strong hydrogen bonds in polar solvents and exist in a *quasi*-molecular state in nonpolar solvents.[12] We have recently shown that small amounts of water in fluorinated ILs, such as 1-butyl-3-methylimidazolium hexafluorophosphate and tetrafluoroborate, have a dramatic effect on the rate of diffusion of ionic and neutral species in these media. It was thus proposed that "wet" ILs may not be regarded as homogeneous solvents but have to be considered as "*nanostructured*" materials, through hydrogen-bond interactions that can possess in some cases polar and nonpolar regions.[13] In this respect, it is also known that imidazolium ILs possess dual behavior when used as a stationary phase for gas chromatography. They act as a low-polarity stationary phase to nonpolar compounds, while molecules with proton donor groups are strongly retained.[14] We have already shown by X-ray studies of 1-*n*-butyl-3-methylimidazolium tetraphenylborate that the hydrogen atoms of the imidazolium ring form three dimension networks through weak C−H−π bonds and that this type of supramolecular structure is maintained to a some extent even in solution, at least in solvents with low dielectric constants, such as chloroform.[15] In this work, we report the X-ray diffraction, ^{1}H NMR, conductivity, and microcalorimetry results

* To whom correspondence should be addressed. E-mail: dupont@iq.ufrgs.br. Fax: +55-5133167304.
† UFRGS.
‡ Present address: Department of Chemistry, UNB, Brasília, DF, Brazil.
§ UFSM.
|| University of Toronto.
⊥ UNICAMP.

10.1021/jp0452709 CCC: $30.25
Published on Web 02/17/2005

CHART 1: 1-*n*-Butyl-3-methylimidazolium-Based ILs

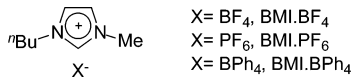

SCHEME 1: Synthesis of the Symmetric Imidazolium ILs

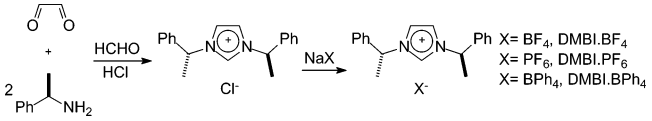

of a series of 1,3-N-disubstituted imidazolium salts, showing that these systems are better described as polymeric supramolecules with weak interactions in pure form, whereas mixtures of imidazolium salts with other molecules may be regarded as nanostructured materials.

Results and Discussion

The Synthesis of 1,3-Dissubstituted Imidazolium-Based ILs. The nonsymmetric 1-*n*-butyl-3-methylimidazolium salts (Chart 1) have been prepared by simple anion metathesis as described previously.[16]

The symmetric 1,3-di-*R*-(+)-methylbenzyl imidazolium cations associated with tetrafluoroborate, hexafluorophosphate, and tetraphenylborate anions have been prepared in good yields (>90%) by the reaction of 2 equiv of *R*-(+)-1-phenetylamine with glyoxal and formaldehyde followed by treatment with hydrochloride acid and anion metathesis (Scheme 1).[17]

Solid-State Structures. The molecular structures of [DMBI]-BF_4, [DMBI]PF_6, and [DMBI]BPh_4 have been investigated by single-crystal X-ray diffraction crystallographic analysis. Diagrams of the structures are shown in Figure 1 for [DMBI]BF_4 and [DMBI]PF_6. Crystallographic data and details of the structure determination are presented in Table 3. Tables of atomic coordinates, hydrogen coordinates, complete list of bond distances and angles, and anisotropic thermal parameters are supplied as Supporting Information.

Figure 1 shows the expected structural features in [DMBI]-BF_4 and [DMBI]PF_6 for the imidazolium cation and the BF_4 and PF_6 anions that are slightly distorted with tetrahedral and octahedral geometries, respectively. Each imidazolium ring is surrounded by three anions, and in turn, each anion is surrounded by three imidazolium cations through hydrogen bonds of the *H*-imidazolium ring with the F atom of the anions. Note that there are also significant hydrogen bonds between the hydrogens of the α-methylbenzyl (MB) *N*-imidazolium substituents and F of the anions. Therefore, when we take into account all of the relevant hydrogen bonds involving the hydrogens of both imidazolium ring and those of the MB *N*-imidazolium substituents, each cation is surrounded by six anions (BF_4 or PF_6). The crystallographic structures of the two salts are quite similar; both resemble a structure previously reported for [BMI]BPh_4.[15] In both compounds, the molecules pack in stacks of cations and anions with an extended network of cations and anions connected by hydrogen bonds (Figure 2).

Table 1 reports the distribution of intermolecular C−H···F angles and H···F distances for [DMBI]PF_6 and [DMBI]BF_4. The BF_4 anion leads to slightly longer C−H···F bonds with respect to the PF_6 anion, while in the PF_6 anion, the C−H donors approach more linearly toward the fluorine.

The nearest interionic interaction was H2−F3 [2.327(3) Å] for [DMBI]BF_4 and H2−F4 [2.204(1) Å] for [DMBI]PF_6, as observed for other 1,3-dialkylimidazolium salts.[19] There are also

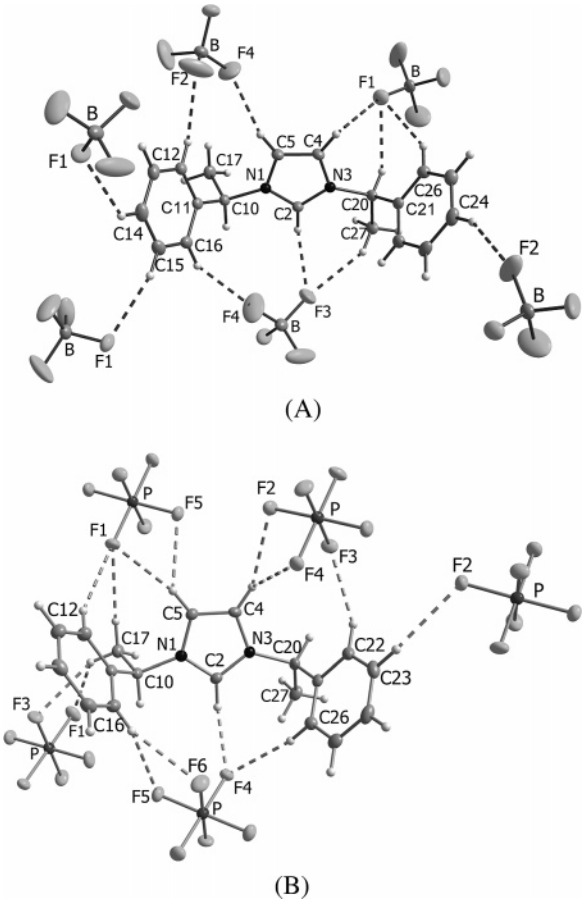

Figure 1. View of the close contacts between the cation and the BF_4 (A) and PF_6 (B) anions (only relevant parts shown) for [DMBI]BF_4 and [DMBI]PF_6 (the sum of van der Waals radii for the H and F atoms is 2.67 Å).[18]

relatively important hydrogen bonds between the methyl group of the benzylic moiety and the fluorine atoms. The most important interactions are 2.448(3) Å (H27A···F3) in [DMBI]-BF_4 and 2.408(4) Å (H26···F4) in [DMBI]PF_6.

Although there are also significant interactions between the hydrogen of the *N*-alkyl hydrogen substituents and the hydrogen of the phenyl ring with the anions, this structural pattern of one cation hydrogen bonded with at least three anions and one anion hydrogen bonded with at least three cations is a general trend for the imidazolium salts[9,15,17,19−24] as pointed out in a recent survey.[25]

This structural pattern is also observed in the case of [DMBI]-BPh_4 in which the interaction between the cation and anion involves weak C−H···π hydrogen bonds (see Figure 3 and Table 2). The crystal of [DMBI]BPh_4 consists of two independent molecules (parts A and B in Figure 3) found in the unit cell. These structures are quite similar to each other, and the conformational feature of the cation that differentiates A and B is the torsion angle of the phenyl moiety around C41−C40−C30−C31 [structure A of Figure 3, 150.29(29)°] or C51−C50−C60−C61 [structure B of Figure 3, 161.68(30)°] of one of the MB side chains.

Although the cation is surrounded by three BPh_4 anions, only one hydrogen of the imidazolium ring has a significant interaction with the anion, while the other hydrogen bonds are resulting from the close contact of the hydrogens of the MB side chains. This is at first glance quite surprising because it is expected that the most important hydrogen bond should involve the most acidic NCHC imidazolium ring as observed in the

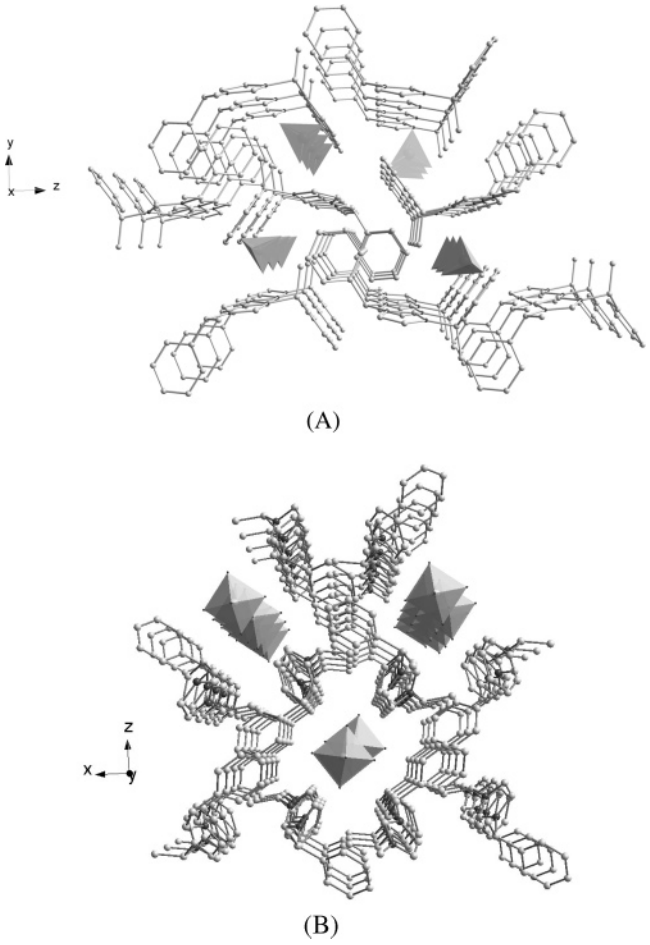

Figure 2. View of the crystal structure of (A) $[DMBI]BF_4$ along the crystallographic *y* axis and (B) $[DMBI]PF_6$ along the crystallographic *z* axis. Hydrogen atoms have been omitted for clarity; BF_4^- and PF_6^- anions are shown as tetrahedra and octahedra, respectively.

structure of the analogous $[BMI]BPh_4$ salt.[15] However, the steric congestion imposed by MB side chains restricts the effective approximation of the phenyl rings of the anions to the NCHN hydrogen to form a hydrogen bond.

The three-dimensional arrangement of the imidazolium cations is formed through chains of the imidazolium rings with weak $\pi\cdots\pi$ stacking interactions. This molecular arrangement generates channels in which the tetraphenylborate anions are accommodated as chains (Figure 4). A similar arrangement was observed in the structure of the analogous $[DMBI]BF_4$ and $[DMBI]PF_6$ salts (Figure 2).

The conformation adopted by the two MB moieties in $[DMBI]BPh_4$ is rather different from those found in compounds of the analogous series $[DMBI]BF_4$ and $[DMBI]PF_6$. The general trend observed in these series was that an increase in anion size reflects a change in conformation of the two MB groups to reach a more efficient packing, from stacked phenyl groups in $[DMBI]BF_4$ to *anti*-position phenyl groups in $[DMBI]BPh_4$. The torsion angles of phenyl groups are 8.67(24)° for $[DMBI]BF_4$ (C21−C20−C10−C11), 28.18(24)° for $[DMBI]PF_6$ (C21−C20−C10−C11), and 161.68(30)° (C51−C50−C60−C61) and 150.29(29)° (C41−C40−C30−C31) for the two independent structures found in $[DMBI]BPh_4$.

The monomeric unit, constituted by at least one cation surrounded by three anions and vice versa, is apparently independent of the nature of imidazolium substituents or on the type of anion (halogen, BF_4, PF_6, BPh_4, etc.). Therefore, the general structural organization of the imidazolium salts in the solid state can be represented as $\{[(DAI)_3(X)]^{2+}[(DAI)(X)_3]^{2-}\}_n$, where DAI is the dialkylimidazolium cation and X is the anion.

TABLE 1: Nearest Hydrogen Interactions in $[DMBI]PF_6$ and $[DMBI]BF_4$

C−H···F	*d*(C−H) (Å)	*d*(H···F) (Å)	*d*(C···F) (Å)	angle (CHF) (deg)
		$[DMBI]PF_6$[a]		
C2−H2···F4	0.95	2.20	3.083(3)	153.5
C4−H4···F2 (a)	0.95	2.58	3.462(3)	154.7
C4−H4···F4 (a)	0.95	2.54	3.171(3)	124.3
C5−H5···F1 (b)	0.95	2.52	3.387(3)	151.0
C5−H5···F5 (b)	0.95	2.56	3.252(3)	130.1
C12−H12···F1 (b)	0.95	2.59	3.468(3)	153.2
C16−H16···F5	0.95	2.64	3.530(3)	155.8
C16−H16···F6	0.95	2.59	3.460(3)	152.8
C17−H17B···F1 (b)	0.98	2.56	3.533(3)	170.9
C17−H17C···F1 (c)	0.98	2.60	3.285(3)	127.1
C17−H17C···F3 (c)	0.98	2.52	3.423(3)	153.6
C22−H22···F3 (a)	0.95	2.64	3.529(3)	155.3
C23−H23···F2 (d)	0.95	2.63	3.512(3)	154.4
C26−H26···F4	0.95	2.41	3.334(3)	164.6
		$[DMBI]BF_4$[b]		
C2−H2···F3	0.95	2.33	3.145(4)	143.8
C4−H4···F1 (a)	0.95	2.58	3.126(3)	116.8
C5−H5···F4 (b)	0.95	2.65	3.320(4)	128.0
C12−H12···F2 (b)	0.95	2.51	3.279(4)	137.6
C14−H14···F1 (c)	0.95	2.53	3.201(4)	127.9
C15−H15···F1 (d)	0.95	2.53	3.387(4)	149.5
C16−H16···F4	0.95	2.45	3.319(4)	151.4
C20−H20···F1 (a)	1.00	2.55	3.352(3)	137.4
C24−H24···F2 (e)	0.95	2.59	3.474(4)	155.9
C26−H26···F1 (a)	0.95	2.57	3.398(3)	146.3
C27−H27A···F3	0.98	2.45	3.306(4)	145.9

[a] Symmetry transformations used to generate equivalent atoms: (a) $x + 1/2, -y + 1/2, -z + 1$; (b) $-x + 1/2, -y + 1, z - 1/2$; (c) $-x, y + 1/2, -z + 3/2$; (d) $-x + 1/2, -y, z - 1/2$. [b] Symmetry transformations used to generate equivalent atoms: (a) $-x + 1/2, -y, z - 1/2$; (b) $-x + 1, y + 1/2, -z + 1/2$; (c) $x + 1, y, z$; (d) $x + 1/2, -y - 1/2, -z + 1$; (e) $-x + 1/2, -y - 1, z - 1/2$.

Solution Structures. Previous ^1H NMR studies showed that $[BMI]BPh_4$ behaves as a contact ion pair in $CDCl_3$ and that these ion pairs form floating aggregates through hydrogen bonds.[15] Figure 5 shows the chemical-shift dependence of the imidazolium hydrogens observed in the ^1H NMR spectra of $[BMI]BPh_4$ and $[DMBI]BPh_4$ in $CDCl_3$ with the concentration.

As can be seen in Figure 5, when we change the *N*-alkyl groups in $[BMI]BPh_4$ for the relatively bulky MB group in $[DMBI]BF_4$, the shielding effect in the imidazolium anions decreases dramatically. This is basically due to the steric hindrance of the MB group, which avoids close contact between the anion and cation, restricting the C−H$\cdots\pi$ interaction. It is noteworthy, that no significant C−H$\cdots\pi$ interaction involving the H2 imidazolium hydrogen was detected in the crystals by X-ray diffraction analysis (Figure 3). However, this C−H$\cdots\pi$ interaction is apparently present in solution and occurs preferentially with the H2 hydrogen in concentrations up to 46 mmol L^{-1}. For higher concentration, H4 and H5 appear downfield to the H2. This result corroborates our previous observations obtained for $[BMI]BPh_4$, for which contact ionic pair formation occurs via H2 in low concentrations and via H4 and H5 for higher concentrations.[15]

Figure 6 shows the H2 chemical-shift dependence with the concentration for $[BMI]BPh_4$ and $[DMBI]BPh_4$ in CD_3CN solutions. The ^1H NMR spectra of $[BMI]BPh_4$ and $[DMBI]BPh_4$ in CD_3CN show signals shifted to higher frequencies than those obtained in $CDCl_3$ (for example, 90 mmol L^{-1} CD_3CN solutions of $[BMI]BPh_4$ and $[DMBI]BPh_4$ shows H2 signals at 8.0 and 8.8 ppm, and in $CDCl_3$ solutions, these peaks appear at 4.4 and

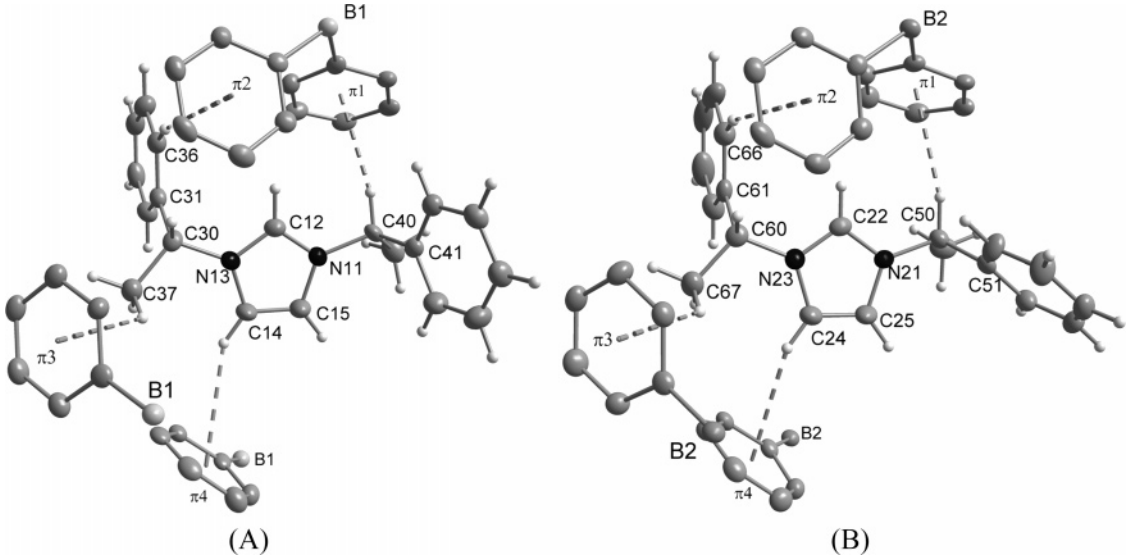

Figure 3. View of the close contacts between the imidazolium cation and the BPh_4 anions (only the relevant parts shown) with the hydrogen bonds with the phenyl centroid indicated (bond distances and angles summarized in Table 2) of the two molecules (A, left, and B, right) founded in the unit cell.

TABLE 2: Nearest C−H···π Ring Interactions in Solid State for [DMBI]BPh_4[a]

C−H···π	d(C−H) (Å)	d(H···π) (Å)	d(C···π) (Å)	angle (CH−π) (deg)
		[DMBI]BPh_4 (A)		
C40−H40···π1	1.00	2.62	3.589(4)	163.8
C36−H36···π2	0.95	2.84	3.749(10)	160.8
C37−H37B···π3 (a)	0.98	2.94	3.521(4)	119.2
C14−H14···π4 (b)	0.95	2.97	3.816(4)	149.1
		[DMBI]BPh_4 (B)		
C50−H50···π1 (c)	1.00	2.71	3.657(4)	157.6
C67−H67C···π3 (d)	0.98	2.79	3.469(4)	126.9
C24−H24···π4 (e)	0.95	2.83	3.713(4)	155.7
C66−H66···π2 (f)	0.95	2.88	3.762(10)	155.9

[a] The centroids are of the following atoms with symmetry operations: (a) $1-x, -0.5+y, 2-z$; (b) $2-x, -0.5+y, 2-z$; (c) $x, -1+y, z$; (d) $1-x, -0.5+y, 1-z$; (e) $2-x, -0.5+y, 1-z$; (f) $x, -1+y, z$.

6.2 ppm). As can be seen in Figure 6, the range of variation of these chemical shifts in CD_3CN with the concentration (0.5 ppm for [BMI]BPh_4 and 0.2 ppm for [DMBI]BPh_4) is not as important as those observed in $CDCl_3$ (up to 1.0 and 0.5 ppm, respectively). These results indicate that, in contrast to $CDCl_3$ solutions, [BMI]BPh_4 and [DMBI]BPh_4 dissolved in CD_3CN behave most probably as solvent separated ion pairs. Noteworthy, evidence for hydrogen bonds between the imidazolium cation and the tetrafluoroborate anion has also been obtained by NMR investigations with [EMI]BF_4 (1-ethyl-3-methylimidazolium tetrafluoroborate) IL[26] and for [BMI]BF_4 in acetonitrile.[27]

The association process shown by ^{1}H NMR can be also conveniently studied by conductometry. The conductivity of the salts solutions, in different compositions was measured at 25 °C using different mixtures of $CHCl_3$ and CH_3CN, to control the dielectric constant of the medium. The behavior of [BMI]-BPh_4 solutions is shown in Figure 7, where the equivalent conductance versus IL concentration in different solvents is plotted.

It can be seen from Figure 7 that the addition of CH_3CN to a $CHCl_3$ solution of [BMI]BPh_4 increases the conductance dramatically. For CH_3CN solutions, the equivalent conductance of the IL solution increases at lower concentrations, as expected for the ionization of the imidazolium salt with the dilution, but in $CHCl_3$ solution, the conductance decreases continuously with the dilution, indicating the existence of equilibrium between a contact ion pair and charged aggregates. At higher salt concentrations, the equivalent conductance in $CHCl_3$ begins to fall as a consequence of higher aggregate formation. Measurements in mixtures of the solvents $CHCl_3$ and CH_3CN, with slightly higher dielectric constants (2.25 acetonitrile wt %), however, show a minimum conductivity point at 3 mmol L^{-1}. This behavior has been described for tetraalkylammonium salts for which a contact ion pair and solvent-separated ion pair equilibria are predominant at low concentrations and equilibria between charged triple ions and ion pairs at higher concentrations.[28]

Scheme 2 shows a simplified model in which different species can coexist in equilibrium at different concentrations. Such multiple-ion formation can explain the conductivity behavior observed with ILs.

With this multiple-ion model it is possible to understand the minimum observed in the equivalent conductivity versus concentration curve, which corresponds to a region where the two equilibria coexist with the same strength. This behavior is not limited to BMI cations. It is also observed for [DMBI]BPh_4, and it is expected to be a general property of imidazolium salts as shown in Figure 8. The equivalent conductivity versus concentration data obtained for [BMI]PF_6, [BMI]BF_4, [DMBI]-PF_6, and [BMI]BF_4 in $CHCl_3/CH_3CN$ 2.8 wt % solutions show identical trends.

The formation of IL aggregates was also investigated by microcalorimetry. At low concentrations (the infinite dilution limit), the solution enthalpies of these compounds may be expressed as the sum of different contributions (eq 1)

$$\Delta H_{sol} = \Delta H_{ion-ion} + \Delta H_{solv-solv} + \Delta H_{ion-solv} \qquad (1)$$

where the first two terms represent, respectively, the enthalpy change for separation of the ions and of the solvent molecules (both positive) and the last one reflects the enthalpy of the ion−solvent interaction, expected to be negative. A positive enthalpy of solution would infer that the sum of the two processes is more energetic than the contribution from ion solvation, and a negative value represents the opposite situation.

As the imidazolium salt concentration is increased, the formation of aggregates may occur, as previously discussed

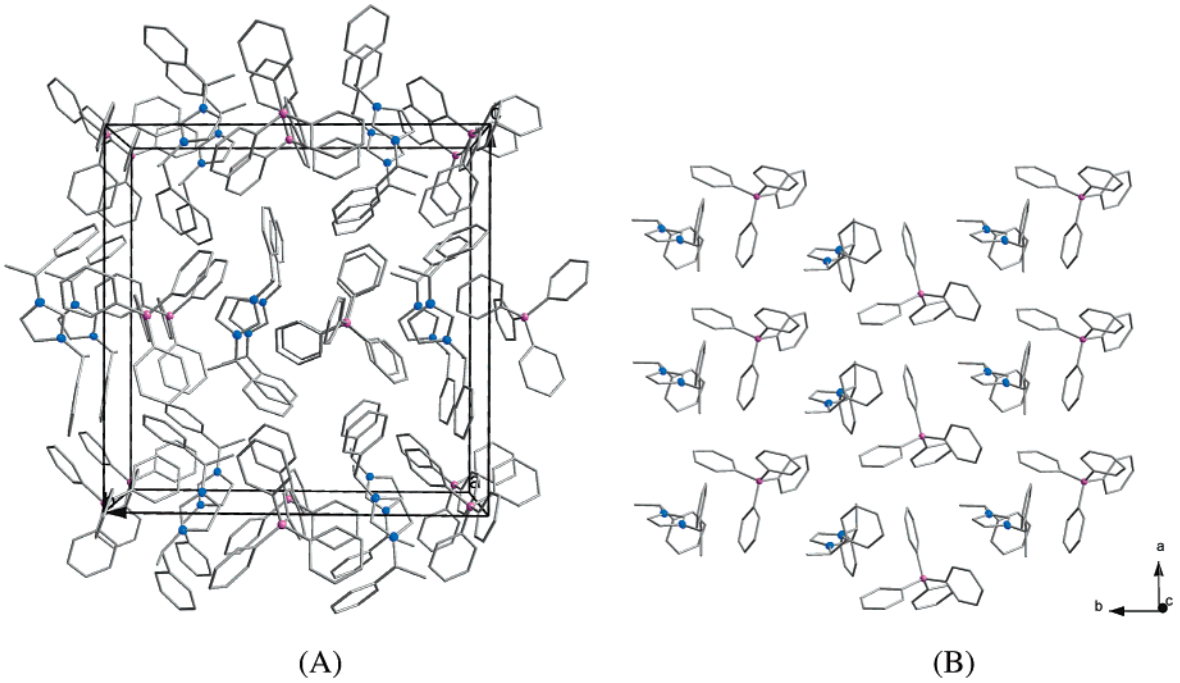

Figure 4. (A) Packing diagram of [DMBI]BPh_4 showing alternating columns parallel to the crystallographic *z* axis of the DMBI cations and BPh_4 anions. (B) Side view of the columns.

TABLE 3: Summary of the Crystal Data and Structure Refinement for [DMBI]BF_4 and [DMBI]PF_6

	[DMBI]BF_4	[DMBI]PF_6	[DMBI]BPh_4
empirical formula	$C_{19}H_{21}BF_4N_2$	$C_{19}H_{21}F_6N_2P$	$C_{43}H_{41}BN_2$
formula weight	364.19	422.35	596.59
temperature	150(2) K	100(2) K	100(2) K
crystal system	orthorhombic	orthorhombic	monoclinic
space group	$P2_12_12_1$	$P2_12_12_1$	$P2_1$
unit cell dimensions	a = 10.7207(3) Å, b = 10.8545(2) Å, c = 15.4841(4) Å	a = 10.2149(5) Å, b = 12.5025(4) Å, c = 15.0057(6) Å	a = 8.484(5) Å, b = 19.347(5) Å, c = 19.586(5) Å, β = 90.506(5)°
volume	1801.85(8) Å^3	1916.40(14) Å^3	3215(2) Å^3
Z	4	4	4
density (calculated)	1.343 Mg/m^3	1.464 Mg/m^3	1.233 Mg/m^3
absorption coefficient	0.107 mm^{-1}	0.207 mm^{-1}	0.070 mm^{-1}
F(000)	760	872	1272
crystal size	0.30 × 0.30 × 0.25 mm^3	0.20 × 0.10 × 0.05 mm^3	
θ range for data collection	2.63−27.49°	4.21−27.49°	2.96−26.35°
index ranges	$-13 < h < 13$, $-14 < k < 14$, $-20 < l < 20$	$-13 < h < 13$, $-16 < k < 16$, $-19 < l < 19$	$0 < h < 10$, $0 < k < 23$, $-23 < l < 23$
reflections collected	22 610	4379	6087
independent reflections	2366 [R(int) = 0.024]	4379 [R(int) = 0.0000]	6087
completeness	99.7%	99.5%	89.9%
absorption correction	multiscan (Denzo-SMN)	multiscan (Denzo-SMN)	multiscan (Denzo-SMN)
maximum and minimum transmission	0.974 and 0.968	0.990 and 0.960	
data/restraints/parameters	2345/0/238	4379/0/257	6087/1/834
goodness-of-fit on F^2	1.042	0.883	1.032
final R indices ($I > 2\sigma(I)$)	$R1$ = 0.0464 w$R2$ = 0.1166	$R1$ = 0.0434 w$R2$ = 0.0736	$R1$ = 0.0461 w$R2$ = 0.1036
R indices (all data)	$R1$ = 0.0530, w$R2$ = 0.1210	$R1$ = 0.0897, w$R2$ = 0.0818	$R1$ = 0.0692, w$R2$ = 0.1112
absolute structure parameter	0.2(13)	0.16(11)	−3(3)
extinction coefficient	0.010(2)	0.0049(7)	0.0125(12)
largest difference peak and hole	0.57 and −0.47 e Å^{-3}	0.210 and −0.192 e Å^{-3}	0.208 and −0.207 e Å^{-3}

based on conductivity and NMR measurements, which will contribute to an increase or decrease of the observed enthalpy of solution. Again, whether ion-pair formation leads to an increase or decrease in the system enthalpy would depend on the balance between ion−solvent interactions (which are being disrupted) and ion−ion interactions (which are being formed). Moreover, previously discussed data have suggested the possibility of further ion association, with the formation of triple ions and higher aggregates, because of hydrogen bonding. These further interactions would add another term to the observed enthalpy of solution (eq 1), which again may lead to an increase or decrease in enthalpy, depending on the balance between interactions that are disrupted and the ones that are formed.

This picture may be better understood by analyzing the data shown in Figures 10 and 11. These data represent the changes of solution enthalpies of four imidazolium salts in chloroform.

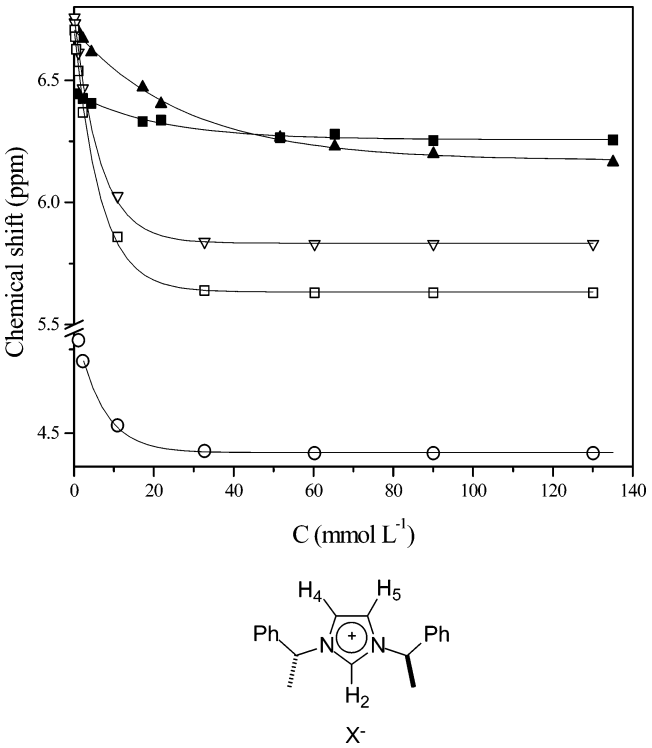

Figure 5. Variation of the ^{1}H NMR chemical shifts of the imidazolium cations with concentration in $CDCl_3$. (▲) H4 and H5 and (■) H2 in $[DMBI]BPh_4$ and (▽) H4, (□) H5, and (○) H2 in $[BMI]BPh_4$.

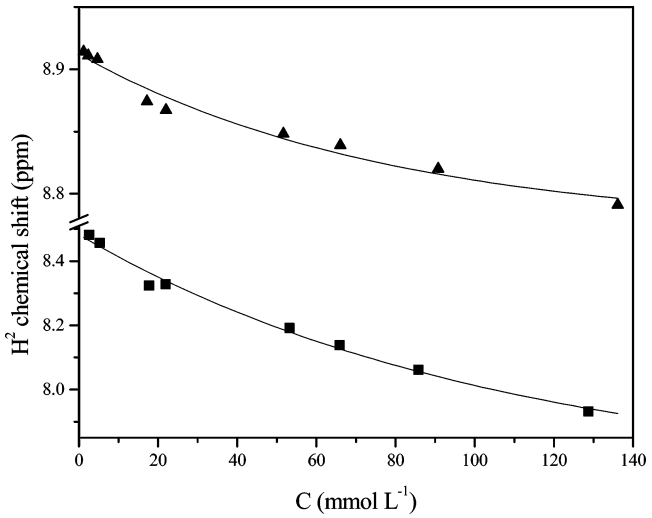

Figure 6. Variation of ^{1}H NMR chemical shifts of the imidazolium cation ($[DMBI]BPh_4$ and $[BMI]BPh_4$) with the concentration in CD_3CN. (■) H2 $[BMI]BPh_4$ and (▲) H2 $[DMBI]BPh_4$.

Apart from the measurements with $[BMI]PF_6$, for which, because of its low solubility, only a few data points could be obtained, all of the other three curves show a constant enthalpy of solution at low concentrations. These values are positive for salts $[DMBI]PF_6$ and $[DMBI]BF_4$, which possess chemically related cations, indicating that the sum of the enthalpies because of the two first processes of eq 1 is greater than the absolute value for the enthalpy change because of ion solvation by chloroform. For $[BMI]PF_6$ and $[BMI]BF_4$, the solution enthalpies are negative, indicating the opposite situation and a more energetic ion solvation. As the concentration increases, these enthalpy values start to change. This occurs at ca. 7, 11, and 60 mmol L^{-1} respectively for $[DMBI]BF_4$, $[DMBI]PF_6$, and $[BMI]BF_4$. Interestingly, these changes occur in an opposite

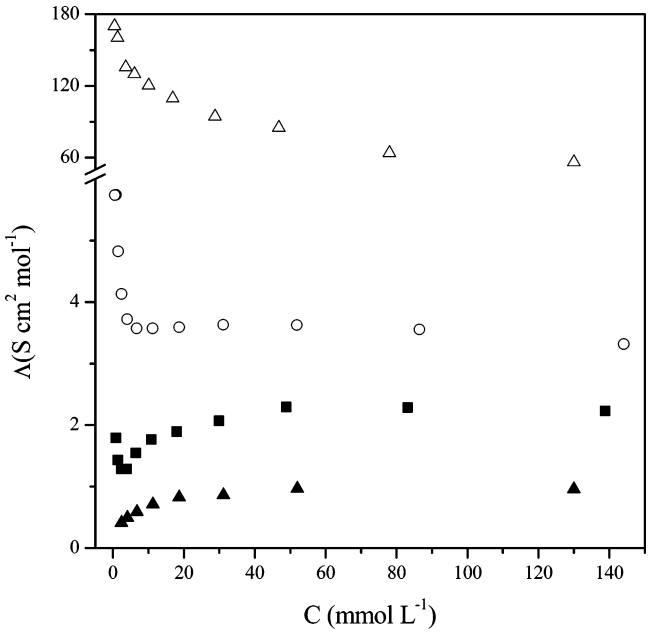

Figure 7. Equivalent conductance of $[BMI]BPh_4$ solutions in (▲) $CHCl_3$, (■) $CHCl_3/CH_3CN$ (2.25 wt % CH_3CN), (○) $CHCl_3/CH_3CN$ (4.45 wt % CH_3CN), and (△) CH_3CN at various IL concentrations.

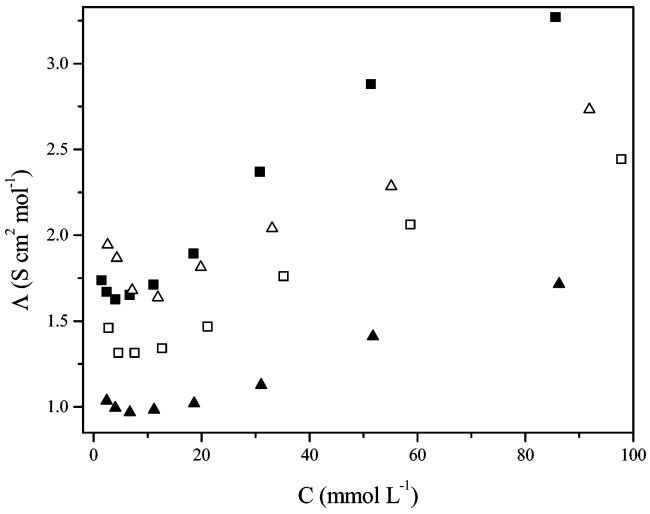

Figure 8. Conductivity of (■) $[BMI]PF_6$, (▲) $[BMI]BF_4$, (△) $[DMBI]PF_6$, and (□) $[DMBI]BF_4$ in $CHCl_3/CH_3CN$ (2.8 wt % in CH_3CN).

direction, leading to lower enthalpy values for the first two imidazolium salts and to an increase in enthalpy for the latter. Again, these trends are consistent with different contributions from solvation and formation of charged triple ions. As the concentration is further increased, another deviation is observed in these curves, reversing the enthalpy variation and suggesting the appearance of another process in solution. According to the previous discussion, we propose that this is the formation of higher aggregates. For $[DMBI]PF_6$ and $[DMBI]BF_4$, the formation of aggregates is detected at ca. 25 mmol L^{-1}, while it is observed at a larger concentration, ca. 110 mmol L^{-1}, for $[BMI]BF_4$.

The data presented in Figure 11, for the solution of $[BMI]BPh_4$ and $[DMBI]BPh_4$ in acetonitrile and chloroform, allow the assessment of solvent contributions to these solution processes. The solution enthalpies measured in acetonitrile are more positive, as a consequence of higher cohesive energy for this more polar solvent, which increases the enthalpy change because of the separation of solvent molecules (as represented

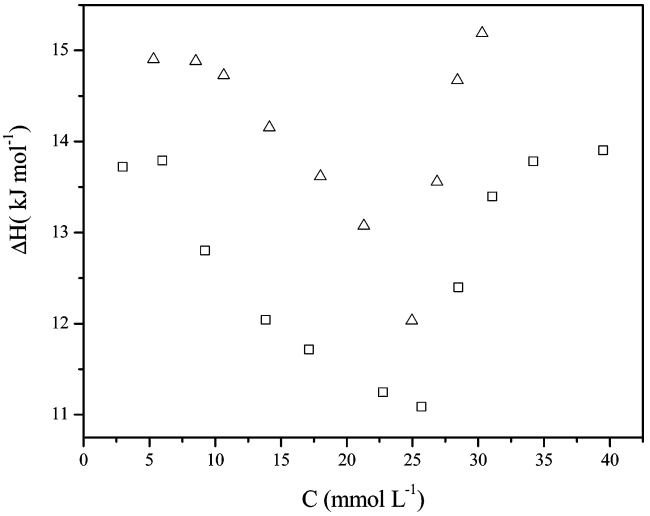

Figure 9. ΔH_{sol} changes of (△) [DMBI]PF_6 and (□) [DMBI]BF_4 in chloroform with the imidazolium salt concentration.

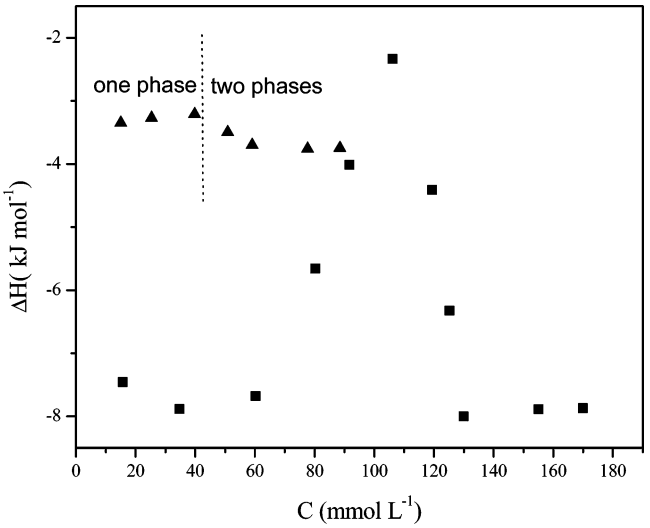

Figure 10. ΔH_{sol} changes of (▲) [BMI]PF_6 and (■) [BMI]BF_4 in chloroform with the imidazolium salt concentration.

in eq 1). The data for solution in chloroform conform to the pattern observed in Figure 9, whereas those obtained in acetonitrile do not show any significant change in solution enthalpies, within the investigated concentration range, suggesting that because of its greater ability to solvate ions (as measured, for instance, by its dielectric constant), no ion pairing is observed.

In summary, 1,3-dialkylimidazolium salts form supramolecules in solid state through hydrogen bonds. The monomeric unit is composed of at least three cations associated with one anion and one cation with at least three anions. These hydrogen-bonded structures are maintained to a great extent even in solution in solvents of low dielectric constant, evidenced through

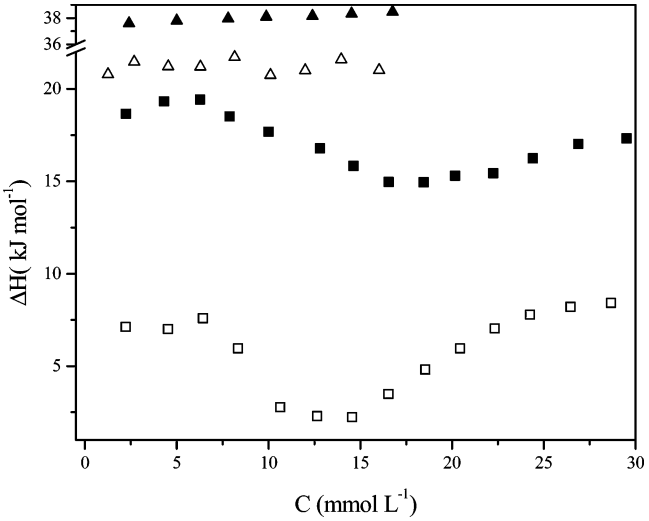

Figure 11. ΔH_{sol} changes of (■) [BMI]BPh_4 and (△) [DMBI]BPh_4 in acetonitrile and (▲) [BMI]BPh_4 and (□) [DMBI]BPh_4 in chloroform.

the detection of supramolecular floating aggregates by NMR, conductometry, and microcalorimetry. Of note is that these structures (possessing mono-, di-, and tricharged species) can be maintained even in the gas phase as observed by fast atomic bombardment (FAB)[29] and electrospray ionization (ESI)[30] mass spectrometry experiments. Therefore, imidazolium ILs mixed with other molecules may be regarded as nanostructured materials. This model, involving supramolecular aggregates, can account for most of the unique physical−chemical properties such as an increase in their electrical conductivity in the presence of nonpolar molecules (carbon dioxide),[31] increasing the diffusion coefficient of both polar and nonpolar compounds by the addition of controlled amounts of water in imidazolium salts,[13] dual behavior when used as a stationary phase for gas chromatography,[14] "polarity",[32] proton transfer "support" properties when used as electrolytes for fuel cells,[33] miscibility with both polar and nonpolar molecules,[34] steric and electronic protecting properties for nanoparticles,[35] stabilization of enzymes,[36] support properties for liquid membranes,[37] the formation of inclusion compounds with aromatic molecules,[38] etc.

Experimental Section

General Considerations. All preparative procedures were carried out under dry argon using standard Schlenk tube techniques. The solvents were distilled from appropriate drying agents under argon. The $NaBPh_4$, $NaBF_4$, and $NaPF_6$ salts were used as purchased from Aldrich Chemical Co. 1-*n*-butyl-3-methylimidazolium chloride,[16] 1-*n*-butyl-3-methylimidazolium tetrafluoroborate,[16] 1-*n*-butyl-3-methylimidazolium hexafluorophosphate,[16] and 1-*n*-butyl-3-methylimidazolium tetraphenylborate[15] were prepared as described earlier. Infrared (Nujol mulls or KBr pellets) spectra were recorded using a Bomem B-102 spectrometer. The ^1H and ^{13}C NMR spectra were

SCHEME 2: Multiple-Ion Equilibria at Different Ionic Concentrations

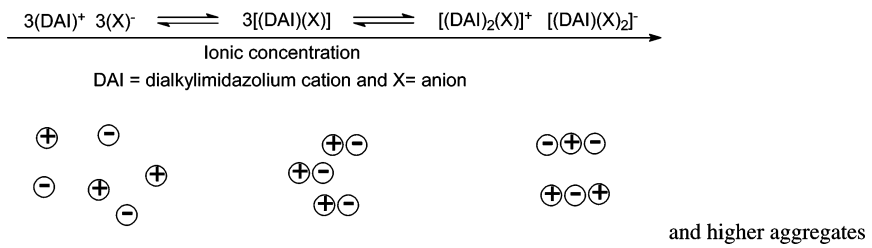

recorded on a Varian Inova 300 instrument. Conductivity measurements were carried out in a Schlenk tube using a commercial platinum electrode calibrated at 298 K by using 1 mol L^{-1} aqueous KCl solution and performed with a CG 859 Schott Gerate Wheatstone bridge.[39] Calorimetric experiments were carried out in a 1200 PL-DSC, under nitrogen flux, with a heating rate varying from 1 to 10 °C. Enthalpies of solution, ΔH_{sol}, for the imidazolium salts in different solvents were measured using the Thermometric 2225 Solution Calorimeter (Thermometric AB, Sweden), operating at 25 °C, according to the instructions of the manufacturer. This unit was inserted into the water bath of another calorimeter (Thermometric 2277), with temperature stability of ±0.0001 °C. Glass ampules were loaded with 3−4 mg of RTIL and sealed by a flame, keeping the ampules under controlled cooling. These ampules were then broken into a 100 mL vial, containing pure solvent or RTIL solution. The measured enthalpy changes were corrected for an almost negligible endothermic effect because of the breaking of ampules, which was discounted based on measurements using empty ampules. Each value reported represents an average of, at least, two measurements. Observed deviations are smaller than 1%. Measuring the solution enthalpies of KCl in water produced values within 0.8% of those in the literature,[40] validating the whole procedure.

Single-crystal determinations were done on a Nonius κ-CCD single-crystal diffractometer with ψ and ω scans with κ offsets using Mo Kα radiation (0.710 73 Å). Data reduction with Lorenz and polarization corrections was made using Denzo/SMN.[41] SIR97[42] or SHELXS[43] were used for data solution, and SHELXL[44] was used for data refinement.

1-3-Di(*R*-(+)-methylbenzyl)imidazolium Chloride ([DMBI]Cl). To a stirred mixture of *R*-(+)-methylbenzylamine (8.3 g, 69.4 mmol) and toluene (20 mL) at 0 °C, formaldehyde (3.95 mL, 34.7 mmol) was added over the course of 10 min. After the addition, the mixture was warmed to room temperature, stirred for 30 min, and lowered again to 0 °C. HCl (2.6 mL, 34.7 mmol) and subsequently glyoxal (2.85 mL, 34.72 mmol) were added to the reaction mixture. After a reflux for 24 h, the solvent was removed in vacuo and 30 mL of dichloromethame was added. After filtration, the solvent was removed in vacuo. The residue was crystallized from acetone at 0 °C. Yield: 70% (7.6 g, 24.3 mmol). Mp = 199 °C. $[\alpha]_D^{25} = +29.8°$ ($C = 1.91$ g/100 mL; CH_2Cl_2). IV (KBr): 3138, 3097, and 3057 cm^{-1} (ν_{C-H} aromatic); 2961, 2924, 2867, and 2801 cm^{-1} (ν_{C-H} aliphatic). ^{1}H NMR ($CDCl_3$): 10.4 (s, 1H, H2); 8.11 (s, 2H, H4 and H5); 7.54 (m, 2H, H*o*); 7.37 (m, 3H, H*m* and H*p*); 5.96 (q, 1H, NCH, $^3J_{HH} = 7.0$ Hz); 1.93 (d, 3H, CH_3, $^3J_{HH} = 7.0$ Hz).^{13}C NMR ($CDCl_3$): 139.6 (C); 134.9 (C2); 128.8 (C*o*); 128.5 (C*m*); 126.6 (C*p*); 121.5 (C4 and C5); 58.6 (NCH); 20.3 (CH_3).

1-3-Di(*R*-(+)-methylbenzyl)imidazolium Tetrafluoroborate ([DMBI]BF_4). Sodium tetrafluoroborate (0.71 g, 6.4 mmol) and 1-3-di(*R*-(+)-methylbenzyl)imidazolium chloride (1.98 g, 6.3 mmol) were diluted in 5 mL of acetone. After stirring at room temperature for 24 h, the sodium chloride was filtered off and the solution was concentrated giving a pale yellow solid. The residue was crystallized from dichloromethane/hexane. Yield: 90% (2.06 g, 5.67 mmol). Mp = 110 °C. $[\alpha]_D^{25} = +17.1°$ ($C = 1.46$ g/100 mL; CH_2Cl_2). IV(KBr): 3176, 3156, 3116, 3098, and 3067 cm^{-1} (ν_{C-H} aromatic); 2988, 2980, and 2935 cm^{-1} (ν_{C-H} aliphatic); 1074 cm^{-1} (ν_{B-F}). ^{1}H NMR ($CDCl_3$): 9.18 (s, 1H, H2); 7.37 (m, 5H, H*o*, H*m*, and H*p*); 7.28 (m, 2H, H4 and H5); 5.73 (q, 1H, NCH, $^3J_{HH} = 6.9$ Hz); 1.94 (d, 3H, CH_3, $^3J_{HH} = 7.0$ Hz). ^{13}C NMR ($CDCl_3$): 137.6 (C); 136.6 (C2); 129.3 (C*o*); 129.2 (C*m*); 126.8 (C*p*); 121.0 (C4 and C5); 60.0 (NCH); 20.5 (CH_3).

1-3-Di(*R*-(+)-methylbenzyl)imidazolium Hexafluorophosphate ([DMBI]PF_6). Potassium hexafluorophosphate (1.16 g, 6.2 mmol) and 1-3-di(*R*-(+)-methylbenzyl)imidazolium chloride (1.9 g, 6.1 mmol) were diluted in 5 mL of acetone. After stirring at room temperature for 24 h, the sodium chloride was filtered off and the solution was concentrated giving a pale yellow solid. The residue was crystallized from dichloromethane/hexane. Yield: 92% (2.37 g, 5.61 mmol). Mp = 108 °C. $[\alpha]_D^{25} = +13.9°$ ($C = 0.22$ g/100 mL; CH_2Cl_2). IV(KBr): 3155, 3109, and 3064 cm^{-1} (ν_{C-H} aromatic); 2995 and 2950 cm^{-1} (ν_{C-H} aliphatic); 841 cm^{-1} (ν_{P-F}); 556 cm^{-1} (δ_{F-P-F}). ^{1}H NMR ($CDCl_3$): 8.82 (s, 1H, H2); 7.38 (m, 5H, H*o*, H*m*, and H*p*); 7.20 (m, 2H, H4 and H5); 5.67 (q, 1H, NCH, $^3J_{HH} = 7.0$ Hz); 1.94 (d, 3H, CH_3, $^3J_{HH} = 7.0$ Hz). ^{13}C NMR ($CDCl_3$): 137.4 (C); 133.2 (C2); 129.4 (C*o* and C*m*); 126.8 (C*p*); 121.1 (C4 and C5); 60.2 (NCH); 20.5 (CH_3).

1-3-Di(*R*-(+)-methylbenzyl)imidazolium Tetraphenylborate ([DMBI]BPh_4). The same procedure was used as for [DMBI]PF_6. [DMBI]BPh_4 was obtained starting from [DMBI]-Cl (1.07 g, 3.26 mmol) and $NaBPh_4$ (1.8 g, 5.2 mmol).Yield: 93% (2.94 g, 4.93 mmol). Mp = 176 °C. $[\alpha]_D^{25} = +16.6°$ ($C = 1.75$ g/100 mL; CH_2Cl_2). IV(KBr): 3153, 3132, 3117, 3080, 3055, 3035, and 3013 cm^{-1} (ν_{C-H} aromatic); 2998 and 2983 cm^{-1} (ν_{C-H} aliphatic). ^{1}H NMR ($CDCl_3$): 7.48 (m, 16H, C*o* and C*m*, BPh_4); 7.42 (m, 5H, H*o*, H*m*, and H*p*, Ph); 6.93 (m, 4H, C*p*, BPh_4); 6.26 (s, 1H, H2); 6.15 (m, 2H, H4 and H5); 4.70 (q, 1H, NCH, $^3J_{HH} = 7.0$ Hz); 1.45 (d, 3H, CH_3, $^3J_{HH} = 7.0$ Hz). ^{13}C NMR ($CDCl_3$): 163.7 (C, BPh_4); 137.3 (C, Ph); 136.0 (C*o*, BPh_4); 132.8 (C2); 129.3 (C*o*, Ph); 129.2 (C*m*, Ph); 126.1 (C*p*, Ph); 125.8 (C*m*, BPh_4); 122.0 (C*p*, BPh_4); 120.2 (C4 and C5); 59.2 (NCH); 21.0 (CH_3).

Acknowledgment. Thanks are due to CNPq, FAPERGS, and FAPESP for partial financial support and to NSERC (Canada) for financial support for the diffractometer. We also thank CNPq for a fellowship to C. S. C.

Supporting Information Available: Tables of full crystal data, atomic coordinates, calculated hydrogen coordinates, anisotropic thermal parameters, a complete list of bond lengths and angles, and CIF files. This material is available free of charge via the Internet at http://pubs.acs.org.

References and Notes

(1) (a) Dupont, J.; de Souza, R. F.; Suarez, P. A. Z. *Chem. Rev.* **2002**, *102*, 3667−3691. (b) Olivier-Bourbigou, H.; Magna, L. *J. Mol. Catal. A: Chem.* **2002**, *182*, 419−437. (c) Dyson, P. J. *Appl. Organomet. Chem.* **2002**, *16*, 495−500. (d) Sheldon, R. *Chem. Commun.* **2001**, 2399−2407. (e) Gordon, C. M. *Appl. Catal., A* **2001**, *222*, 101−117. (f) Wasserscheid, P.; Keim, W. *Angew. Chem., Int. Ed.* **2000**, *39*, 3773−3789.

(2) (a) Suarez, P. A. Z.; Dullius, J. E. L.; Einloft, S.; de Souza, R. F.; Dupont, J. *Polyhedron* **1996**, *15*, 1217−1219. (b) Chauvin, Y.; Mussmann, L.; Olivier, H. *Angew. Chem., Int. Ed. Engl.* **1996**, *34*, 2698−2700.

(3) Dupont, J.; Spencer, J. *Angew. Chem., Int. Ed.* **2004**, *43*, 5296−5297.

(4) For the structure and physical−chemical properties of imidazolium ionic liquids, see: (a) Suarez, P. A. Z.; Selbach, V. M.; Dullius, J. E. L.; Einloft, S.; Piatnicki, C. M. S.; Azambuja, D. S.; de Souza, R. F.; Dupont, J. *Electrochim. Acta* **1997**, *42*, 2533−2535. (b) Suarez, P. A. Z.; Einloft, S.; Dullius, J. E. L.; de Souza, R. F.; Dupont, J. *J. Chim. Phys. Phys.-Chim. Biol.* **1998**, *95*, 1626−1639. (c) Ngo, H. L.; LeCompte, K.; Hargens, L.; McEwen, A. B. *Thermochim. Acta* **2000**, *357*, 97−102. (d) Seddon, K. R.; Stark, A.; Torres, M. J. *Pure Appl. Chem.* **2000**, *72*, 2275−2287.

(5) Zhao, H.; Malhotra, S. V. *Aldrichimica Acta* **2002**, *35*, 75−83.

(6) For instance, see: (a) McEwen, A. B.; Ngo, H. L.; LeCompte, K.; Goldman, J. L. *J. Electrochem. Soc.* **1999**, *146*, 1687−1695. (b) Boxall, D. L.; Osteryoung, R. A. *J. Electrochem. Soc.* **2002**, *149*, E185−E188.

(7) See for example: Visser, A. E.; Swatloski, R. P.; Griffin, S. T.; Hartman, D. H.; Rogers, R. D. *Sep. Sci. Technol.* **2001**, *36*, 785−804.

(8) (a) Fannin, A. A., Jr.; Floreani, D. A.; King, L. A.; Landers, J. S.; Piersma, B. J.; Stech, D. J.; Vaughn, R. L.; Wilkes, J. S.; Williams, J. L. *J. Phys. Chem.* **1984**, *88*, 2614−2621. (b) Consorti, C. S.; de Souza, R. F.; Dupont, J.; Suarez, P. A. Z. *Quim. Nova* **2001**, *24*, 830−837. (c) Larsen, A. S.; Holbrey, J. D.; Tham, F. S.; Reed, C. A. *J. Am. Chem. Soc.* **2000**, *122*, 7264−7272. (d) Holbrey, J. D.; Seddon, K. R. *J. Chem. Soc., Dalton Trans.* **1999**, 2133-2139. (e) Bonhote, P.; Dias, A. P.; Papageorgiou, N.; Kalyanasundaram, K.; Gratzel, M. *Inorg. Chem.* **1996**, *35*, 1168−1178. (f) Hitchcock, P. B.; Seddon, K. R.; Welton, T. *J. Chem. Soc., Dalton Trans.* **1993**, 2639−2643.

(9) Dymek, C. J., Jr.; Grossie, D. A.; Fratini, A. V.; Adams, W. W. *J. Mol. Struct.* **1989**, *213*, 25−34.

(10) Golovanov, D. G.; Lyssenko, K. A.; Antipin, M. Y.; Vygodskii, Y. S.; Lozinskaya, E. I.; Shaplov, A. S. *Cryst. Growth Design* **2005**, *5*, 337−340.

(11) (a) Hayashi, S.; Ozawa, R.; Hamaguchi, H. *Chem. Lett.* **2003**, *32*, 498−499. (b) Ozawa, R.; Hayashi, S.; Saha, S.; Kobayashi, A.; Hamaguchi, H. *Chem. Lett.* **2003**, *32*, 948−949. (c) Hardacre, C.; Holbrey, J. D.; McMath, S. E. J.; Bowron, D. T.; Soper A. K. *J. Chem. Phys.* **2003**, *118*, 273−278.

(12) Avent, A. G.; Chaloner, P. A.; Day, M. P.; Seddon, K. R.; Welton, T. *J. Chem. Soc., Dalton Trans.* **1994**, 3405−3413.

(13) Schroder, U.; Wadhawan, J. D.; Compton, R. G.; Marken, F.; Suarez, P. A. Z.; Consorti, C. S.; de Souza, R. F. and Dupont, J. *New J. Chem.* **2000**, *24*, 1009−1015.

(14) Armstrong, D. W.; He, L. F.; Liu, Y. S. *Anal. Chem.* **1999**, *71*, 3873−3876.

(15) Dupont, J.; Suarez, P. A. Z.; de Souza, R. F.; Burrow, R. A.; Kintzinger, J. P. *Chem.—Eur. J.* **2000**, *6*, 2377−2381.

(16) Dupont, J.; Consorti, C. S.; Suarez, P. A. Z.; de Souza, R. F. *Org. Synth.* **2002**, *79*, 236−243.

(17) (a) Arduengo, A. J., III; U.S. Patent 5077414, 1991. (b) Herrmann, W. A.; Goossen, L. J.; Artus, G. R. J.; Kocher, C. *Organometallics* **1997**, *16*, 2472−2477.

(18) Bondi, A. *J. Phys. Chem.* **1964**, *68*, 441−451.

(19) Fuller, J.; Carlin, R. T.; Delong, H. C.; Haworth, D. *J. Chem. Soc., Chem. Commun.* **1994**, 299−300.

(20) Holbrey, J. D.; Reichert, W. M.; Nieuwenhuyzen, M.; Johnston, S.; Seddon, K. R.; Rogers, R. D. *Chem. Commun.* **2003**, 1636−1637.

(21) Saha, S.; Hayashi, S.; Kobayashi, A.; Hamaguchi, H. *Chem. Lett.* **2003**, *32*, 740−741.

(22) Swatloski, R. P.; Holbrey, J. D.; Rogers, R. D. *Green Chem.* **2003**, *5*, 361−363.

(23) Elaiwi, A.; Hitchcock, P. B.; Seddon, K. R.; Srinivasan, N.; Tan, Y. M.; Welton, T.; Zora, J. A. *J. Chem. Soc., Dalton Trans.* **1995**, 3467−3472.

(24) Gordon, C. M.; Holbrey, J. D.; Kennedy, A. R.; Seddon, K. R. *J. Mater. Chem.* **1998**, *8*, 2627−2636.

(25) Dupont, J. *J. Braz. Chem. Soc.* **2004**, *15*, 341−350.

(26) Huang, J. F.; Chen, P. Y.; Sun, I. W.; Wang, S. P. *Inorg. Chim. Acta* **2001**, *320*, 7−11. (b) Huang, J. F.; Chen, P. Y.; Sun, I. W.; Wang, S. P. *Spectrosc. Lett.* **2001**, *34*, 591−603.

(27) Mele, A.; Tran, C. D.; Lacerda, S. H. P. *Angew. Chem., Int. Ed.* **2003**, *42*, 4364−4366.

(28) See for example: (a) Abbott, A. P.; Schiffrin, D. J. *J. Chem. Soc., Faraday Trans.* **1990**, *86*, 1453−1459. (b) Fuoss, R. M.; Kraus, C. A. *J. Am. Chem. Soc.* **1957**, *79*, 3304−3310. (c) Fuoss, R. M.; Kraus, C. A. *J. Am. Chem. Soc.* **1933**, *55*, 21−37. (d) Fuoss, R. M.; Kraus, C. A. *J. Am. Chem. Soc.* **1933**, *55*, 476−488.

(29) AbdulSada, A. K.; Elaiwi, A. E.; Greenway, A. M.; Seddon, K. R. *Eur. Mass Spectrom.* **1997**, *3*, 245−247.

(30) (a) Dyson, P. J.; McIndoe, J. S.; Zhao, D. B. *Chem. Commun.* **2003**, 508−509. (b) Gozzo, F. C.; Santos, L. S.; Augusti, R.; Consorti, C. S.; Dupont, J.; Eberlin, M. N. *Chem.—Eur. J.* **2004**, *10*, 6187−6193.

(31) Zhang, J. M.; Yang, C. H.; Hou, Z. S.; Han, B. X.; Jiang, T.; Li, X. H.; Zhao, G. Y.; Li, Y. F.; Liu, Z. M.; Zhao, D. B.; Kou, Y. *New J. Chem.* **2003**, *27*, 333−336.

(32) (a) Baker, S. N.; Baker, G. A.; Bright, F. V. *Green Chem.* **2002**, *4*, 165−169. (b) Aki, S. N. V. K.; Brennecke, J. F.; Samanta, A. *Chem. Commun.* **2001**, 413−414. (c) Carmichael, A. J.; Seddon, K. R. J. *Phys. Org. Chem.* **2000**, *13*, 591−595.

(33) (a) Susan, M. A. B. H.; Noda, A.; Mitsushima, S.; Watanabe, M. *Chem. Commun.* **2003**, 938−939. (b) de Souza, R. F.; Padilha, J. C.; Gonçalves, R. S.; Dupont, J. *Electrochem. Commun.* **2003**, *5*, 728−731.

(34) (a) Dullius, J. E. L.; Suarez, P. A. Z.; Einloft, S.; de Souza, R. F.; Dupont, J.; Fischer, J.; De Cian, A. *Organometallics* **1998**, *17*, 815−819. (b) Dyson, P. J.; Ellis, D. J.; Welton, T. *Can. J. Chem.* **2001**, *79*, 705−708. (c) Anthony, J. L.; Maginn, E. J.; Brennecke, J. F. *J. Phys. Chem. B* **2002**, *106*, 7315−7320. (d) Cammarata, L.; Kazarian, S. G.; Salter, P. A.; Welton, T. *Phys. Chem. Chem. Phys.* **2001**, *3*, 5192−5200. (e) Gutowski, K. E.; Broker, G. A.; Willauer, H. D.; Huddleston, J. G.; Swatloski, R. P.; Holbrey, J. D.; Rogers, R. D. *J. Am. Chem. Soc.* **2003**, *125*, 6632−6633. (f) Hanke, C. G.; Johanson, A.; Harper, J. B.; Lynden-Bell, R. M. *Chem. Phys. Lett.* **2003**, *374*, 85−90 and references therein.

(35) (a) Dupont, J.; Fonseca, G. S.; Umpierre, A. P.; Fichtner, P. F. P.; Teixeira, S. R. *J. Am. Chem. Soc.* **2002**, *124*, 4228−4229. (b) Huang, J.; Jiang, T.; Han, B. X.; Gao, H. X.; Chang, Y. H.; Zhao, G. Y.; Wu, W. Z. *Chem. Commun.* **2003**, 1654−1655. (c) Fonseca, G. S.; Umpierre, A. P.; Fichtner, P. F. P.; Teixeira, S. R.; Dupont, J. *Chem.—Eur. J.* **2003**, *9*, 3263−3269. (d) Scheeren, C. W.; Machado, G.; Dupont, J.; Fichtner, P. F. P.; Texeira, S. R. *Inorg. Chem.* **2003**, *42*, 4738−4742. (e) Silveira, E. T.; Umpierre, A. P.; Rossi, L. M.; Machado, G.; Morais, J.; Soares, G. V.; Baumvol, I. L. R.; Teixeira, S. R.; Fichtner, P. F. P.; Dupont, J. *Chem.—Eur. J.* **2004**, *10*, 3734−3740. (f) Antonietti, M.; Kuang, D. Smarsly, B.; Zhou, Y. *Angew. Chem., Int. Ed.* **2004**, *43*, 4988−4992.

(36) Lozano, P.; de Diego, T.; Carrie, D.; Vaultier, M.; Iborra, J. L. *Biotech. Prog.* **2003**, *19*, 380−382.

(37) Branco, L. C.; Crespo, J. G.; Afonso, C. A. M. *Angew. Chem., Int. Ed.* **2002**, *41*, 2771−2773.

(38) Holbrey, J. D.; Reichert, W. M.; Nieuwenhuyzen, M.; Sheppard, O.; Hardacre, C.; Rogers, R. D. *Chem. Commun.* **2003**, 476−477.

(39) Jones, G.; Bradshaw, B. C. *J. Am. Chem. Soc.* **1933**, *55*, 1780−1800.

(40) Parker, V. B. *Thermal Properties of Aqueous Solutions of Univalent Electrolytes*, U.S. Government Printing Office, Washington, DC, 1965.

(41) Otwinowski, Z.; Minor, W. *Methods Enzymol.* **1997**, *276*, 307−326.

(42) Altomare, A.; Burla; M. C.; Camalli; M.; Cascarano, G.; Giacovazzo, C.; Guagliardi, A.; Moliterni, A. G. G.; Polidori, G.; Spagna; R. *J. Appl. Crystallogr.* **1999**, *32*, 115−119.

(43) Sheldrick, G. M. *Acta Crystallogr., Sect. A* **1990**, *46*, 467−473.

(44) Sheldrick, G. M. *SHELXL97*; University of Goëttingen, Goëttingen, Germany, 1997.